Journal Homepage: - www.journalijar.com

INTERNATIONAL JOURNAL OF ADVANCED RESEARCH (IJAR)

Article DOI: 10.21474/IJAR01/18638
DOI URL: http://dx.doi.org/10.21474/IJAR01/18638

RESEARCH ARTICLE

STRUCTURAL AND OPTICAL CHARACTERISTICS OF POLY (VINYL ALCOHOL) (PVA)/ ZIRCONIUM OXIDE (ZRO_2) COMPOSITE FILMS

S. Abdel Aal and Murshidah
Department of Physics, College of Science, Qassim University, Buraydah 51452, Saudi Arabia.

Manuscript Info

Manuscript History
Received: 28 February 2024
Final Accepted: 31 March 2024
Published: April 2024

Abstract

Nanocomposite membranes of ZrO_2-doped polyvinyl alcohol (PVA) with varying amounts of ZrO_2 nanoparticles (1, 2, 3 and 5 wt%) have been prepared via a solution casting technique. The ZrO_2 nanoparticles are used as a filler synthesized by sol–gel technique. Effects of ZrO_2 nanoparticles doping on composites' morphological, structural and optical characteristics have been analyzed by X-ray diffraction (XRD), UV–visible spectroscopy, Fourier transform infrared spectroscopy,. The XRD studies confirm the successful incorporation of ZrO_2 into the PVA matrix and showed improved crystallinity following the doping of ZrO_2 in PVA. The UV–visible studies of nanocomposite films show an enhancement in absorption intensity and a slight red shift in peak positions as the ZrO_2 concentration increases. The enhancement in absorption intensity suggests the potential applications in filters and solar cells.

Introduction:-

Polymer nanocomposite is a combination of materials that use polymer as the matrix and nanomaterials as the filler.

Typically, polymer properties are modified by the addition of nanofillers into the polymer matrix[1]. The blending of polymers may result in reducing their basic cost, improving their processing, and maximizing their important properties. Thus, during the past few years, researchers have paid considerable attention to the study of polymer composite. There are several methods for the preparation of polymer blends, but among them, solution blending is very simple and rapid method because it requires simple equipment and not involved any complicated process.

Among all the various polymers, special attentions have been focused on polyvinyl alcohol (PVA)-based nanocomposites, because the transparency of PVA remains unaltered on addition of nanoparticles .

Poly (vinyl alcohol) (PVA) is a semicrystalline and water-soluble polymer with nontoxic, better film-forming, excellent chemical resistance, biocompatible, and good mechanical properties. It is a biodegradable synthetic polymer which has been utilized for many industrial applications, such as paper coating, paper processing, flexible water-soluble packaging films, textile sizing, finishing adhesives, and dispersant agent[2]. Polymeric composite has new characteristics that would not be possible with the individual components caused by their interaction.

PVA were modified by adding a variety of fillers to enhance its, physical and optical, properties.

Corresponding Author:- S. Abdel Aal
Address:- Department of Physics, College of Science, Qassim University, Buraydah 51452, Saudi Arabia.

PVA and its composite structures are used in a variety of sensors, such as humidity, gas, strain, dew, carbon, piezoresistive, optical, and radiation sensors. The carbon chain backbone of PVA has hydroxyl groups attached, which facilitates hydrogen bonding in polymer composites.

Wide bandgap metal oxide ZrO_2 (zirconia) has potential use in various science and technology fields. It exhibits admirable thermal, electrical, optical, and mechanical properties, such as low thermal conductivity, high refractive index, optical transparency, high hardness, high fracture toughness, excellent corrosion resistance, and polymorphic characteristics!" Due to its useful properties, ZrO_2 nanoparticles have wide applications in ceramics, catalysts, gas sensors, solid-state electrolytes, fuel cell, optical devices, and protective coatings. They are widely used as drug delivery carriers for some medicines like penicillin, as gene delivery vehicles with target specificity for some tissues for improving the properties of traditional bone cements also ZrO_2 is a neutral bio ceramic material. The usefulness of Zirconium oxide nanoparticles depends on their size and physical properties in addition to their chemical composition There are three different phases exhibited in pure ZrO_2, namely, monoclinic, tetragonal, and cubic phase.

Incorporating ZrO_2 nanoparticles into PVA can enhance PVA optical and physical properties due to strong interfacial interaction between ZrO_2 nanoparticles and PVA, as reported by J. Selvi et al[1, 3]. The optical transmission of the studied composite films decreased rapidly by increasing the ratio of ZrO_2. This is ascribed to the production of levels in the band via raising the dopant weight, which led to a reduction in transmission and improves in absorption, signifying a variance in the optical gap. The composite film PVA/ZrO_2 is totally blocked in the UV–vis light range between 190 and ~ 650 nm and is totally blocked in the complete range of UV-vis light. For this reason, composite PVA/ZrO_2 films are appropriate for CUT – OFF laser filter applications.

The addition of ZrO_2 particles in the matrix of PVA related to light absorbance/scattering in the UV region. ZrO_2 is considered an actively and typically photocatalyst and photon absorber among wide band metal oxides. Due to their configuration (Zr^{4+} ion is d0), d-d transitions cannot occur in the vision area Then, composite films are more absorbed with increasing ZrO_2 concentration. This is because the addition of ZrO_2 particles absorbs the radiation incident through its free electrons and this agree with [4].

In the present work, we report a versatile solution casting technique for the preparation of PVA/ZrO_2, nanocomposite films. Four different samples of PVA/ZrO_2, composite were fabricated using varying amounts of ZrO_2, nanoparticles (1, 2, 3and 5 wt.%) with respect to PVA. The effect of varying amounts of ZrO_2 nanoparticles on the structural and optical characteristics of composites has been explored to assess a suitable material for optical and optoelectronic applications.

Experimental work

PVA (MW - 85 000-124 000) was procured from Center of radiation research and technology. Zirconium (IV) tetrachloride was used as a zirconium precursor purchased from Sigma-Aldrich. Deionized water was used as a solvent. Ethanol and ammonium solution (NHOH) were also purchased from Sigma-Aldrich

ZrO_2 Nanoparticles preparation

We prepared ZrO_2 nanoparticles using the sol-gel method. For obtaining ZrO_2, nanoparticles, zirconium tetrachloride was dissolved in deionized water (100 mL) under constant stirring on a magnetic stirrer for 30 min and then maintaining a pH of 7-8 by slowly adding NH_4OH solution.

To enhance aging, the reaction mixture was kept at room temperature overnight under continuous constant stirring and after that centrifuged to remove water. The samples were washed with water and ethanol and filtered with filter paper. The recovered gel was dried at 70 °C then crushed to get fine powder and calcined at 700 °C for 2 h to obtain ZrO_2 nanoparticles.

Preparation of PVA and PVA/ZrO_2 Composite films

We used a solution casting technique for the preparation of PVA and PVA/ZrO_2, nanocomposite films with various loading of ZrO_2 nanoparticles (1, 2,3 and 5 wt.%). A pure and homogeneous solution of PVA was obtained by dissolving 1 g of PVA into 10mL deionized water and stirring vigorously at 80°C until transparent solution. For example, At the same time, ZrO_2 nanoparticles (1 wt.%) were dispersed in 10 mL of deionized water separately at ambient temperature for 3 h and then added with

PVA solution. The solution was again stirred for 1h with the magnetic stirrer for 2hours. The resulting PVA-ZrO_2 solution was poured on clean dried Petri dish and left to dry for 2 days at room temperature. The dried PVA/ZrO_2 (1 wt.%) composite films was peeled off from the Petri dish and cut into the required size for further analysis. The same process was also repeated for the preparation of PVA/ZrO_2 (1 wt.%), PVA/ZrO_2 (2 wt.%), PVA/ZrO_2 (3 wt.%), and PVA/ZrO_2 (5 wt.%) composite films.

Result and Discussion:-

The composite films were prepared using a solution casting method, where PVA and ZrO_2 nanoparticles were mixed in different weight ratios. The films were then characterized using various techniques to understand their structural and optical properties.

Structural Characterization

X-Ray Diffraction (XRD) Analysis

In order to understand the properties of composite material, it is essential to know about the details of its structure; The X-ray diffraction (XRD) technique was used for phase analysis. The XRD of PVA, ZrO_2 and PVA/ZrO_2 composites were recorded using Philips X'PERT PRO diffractometer with Cu Kα (λ= 1.54060 Å) incident radiation. The XRD peaks were recorded in the 2θ range of 10°–70°.

Fig.1. XRD pattern (a) of prepared pure PVA film

Fig.2. XRD pattern (b) of prepared pure ZrO_2 powder

Fig.3. XRD pattern (c) of prepared PVA/ZrO_2 sheet with PVA/ZrO_2 (1 wt.%)

Fig.4. XRD pattern (d)of prepared PVA/ZrO_2 sheet with PVA/ZrO_2 (2 wt.%)

Fig.5. XRD pattern (e) of prepared PVA/ZrO_2 sheet with PVA/ZrO_2 (3 wt.%)

Fig.6 .XRD pattern (f)of prepared PVA/ZrO_2 sheet with PVA/ZrO_2 (5 wt.%)

Fig.7. XRD pattern of prepared PVA/ZrO_2 composite film with different ratios of ZrO_2 (a - 0Wt% ZrO_2 , b -1Wt% ZrO_2 , c -2Wt% ZrO_2 , d -3Wt% ZrO_2, and e-5Wt% ZrO_2 5wt.%)

XRD patterns of pure PVA, ZrO_2 and PVA/$ZrO_2$with different ratios of ZrO_2 are shown in Figs. (1-7). The PVA pattern in fig.1.a exhibits a diffraction peak located at 2θ =20.435◦ and a minor tiny peak at 2θ =42.185° which corresponds to (m-022) crystal reflection plane of PVA representing the semicrystalline nature of the PVA due to

strong intermolecular hydrogen bonding between the PVA molecular chains and this results agree and reported with And The XRD pattern of the prepared ZrO_2 sample calcined at 700 °C illustrated in Fig.2.b All the prominent peaks are identified according to JCPDS card no. 88-1007. A summary of peak positions, corresponding to Miller indices, for pure PVA and ZrO_2 are given in Tables 1.

The XRD pattern shows diffraction peaks at 2θ = 30.215°, 35.01° , 50.375° and 59°.125, corresponding to the (101), (110), (112), and (211), planes ZrO_2, is found to be in the tetragonal phase as indicated by the indexed XRD peaks. In addition to monoclinic peak at 2θ=40.825° corresponding to plane (021) [JCPDS-17-923].

In fig.3. the composite film prepared with ratio 1wt % ZrO_2 shows characteristic diffraction peaks of ZrO_2 nanoparticles with the PVA polymer, revealing that the ZrO_2 nanoparticles are incorporated in PVA host. As can be seen, a notable decrease of broadening in the PVA diffraction peak intensity were detected, this can be related the H–bond and –OH group of the PVA chains may break and molecular chains are free to rotate. In addition, the PVA peak at 20.435^o was shifted to lower angle side to 20.341 ^{o} This may be related to the intermolecular interaction between the PVA chains and ZrO_2 particles, affecting the composite crystallinity. The slight broadening of the peaks of ZrO_2 and increase of crystal size as show in fig.8. and table 2 may also be attributed to the micro-strain of the crystal structure arising from defects like dislocation due to the formation of weak bonds with the PVA polymer.

At figs.4. and fig.5. with ratios 2 and 3 wt.%, ZrO_2 diffraction peaks get narrower and sharper with higher intensity. In addition, a slight shift to low angel in the PVA peaks to 19.985^o, 19.925 ^{o}, respectively and ZrO_2 diffraction peaks to lower angle side was also observed. This indicates that their combination at the PVA/ZrO_2 interface reduce the intermolecular stress in the amorphous portions, consequently increasing the mobility of the PVA chain allowing the reordering of particular molecules, thus improving the composite crystallinity.

Fig.6. represent the XRD pattern of PVA/ZrO_2 composite film with ratio 5wt.% revealing the diffraction peaks at 2= 29.825° 34.775°, 40.787° 49.265°, and 58.685° correspond to the ZrO_2 dopant, however, the peak located at 19.836° revealed the characteristic diffraction peak of PVA. The diffraction peaks of the PVA/ ZrO_2, composite film shifted to lower angles than that of the pure PVA film, due to the that successfully incorporated ZrO_2, nanoparticles into the PVA matrix. And this agrees with (20,21), The broad hump (10–20°) also decreased upon the addition of zirconia, which points to the improvement of crystallinity in the host polymer PVA.

The Scherrer's relation, D= K /βcosθ. was used to determine the average crystallite size of pure PVA and PVA doped with ZrO_2, as show in table 2 and fig.8. where D is the crystallite size along k = 0.9 is the fixed number, β is FWHM of the diffraction peak , is the wavelength of X -ray (λ= 1.54060 Å), and θ is the Bragg angle, The calculated average value of crystallite size for pure PVA and PVA doped with ZrO_2 was found to be 27.63607, 27.9166, 28.09502, 29.42043 and 29.961 Nm. The estimated the average value of crystallites size is about (27.636-29.961nm)[5]. The dislocation density (δ) was calculated from Williamson and Smallman's formula:

(1)

where "n" is a factor, which when equal to unity gives the minimum dislocation density, and "D" is the average crystallite size. The average micro strain (ε) developed in the as-prepared nano composite films was calculated by using the relation:

(2)

where β is the full width at half maximum and θ is the Bragg angle. It has been observed that the dislocation density and micro- strain decrease with increase in crystallite size, as shown in figs (8,9) which indicates a lower number of lattice imperfec- tions. This may be due to a decrease in the occurrence of grain boundaries because of an increase in the crystallite size of the film with increasing ZrO_2 ratios may be due to the improvement in the crystallinity of the film[6].

Table 1:- A summary of peak positions, corresponding full width half maximum, peak intensities, miller indices, and particle size for pure PVA and ZrO_2 particles.

sample	2theta	h k l
ZrO2(a)	30.215 ^{o}	101
	35.01 ^{o}	110
	40.885 ^{o}	021

	50.375 ^{o}	112
	59.125 ^{o}	211
PVA	20.43 ^{o}	111
	41.852 ^{o}	022

Table 2:- A summary of peak positions, FWHM, and particle size for PVA/ZrO_2 composite films.

sample PVA/ZrO_2	2theta	FWHM PVA/ZrO_2	Crystal (D)size Nm	Dislocation density(lines/m^2)	Micro-strain ($x10^{-6}$)
0%	20.43 ^{o}	2.93	27.6360712	0.00130932	0.72085325
1%	20.341 ^{o}	2.9	27.9166284	0.00128314	0.7136088
2%	19.985 ^{o}	2.88	28.0950233	0.0012669	0.7090776
3%	19.925 ^{o}	2.75	29.4204332	0.00115532	0.67713319
5%	19.836 ^{o}	2.7	29.9611798	0.00111399	0.66491213

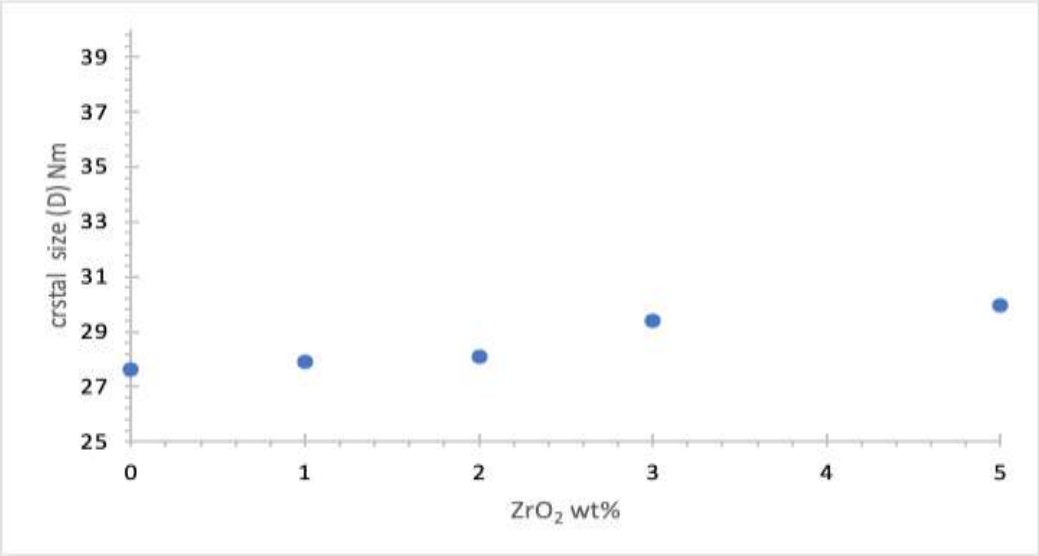

Fig.8:- Effect of ZrO_2 ratios on the crystal size of nano composite films.

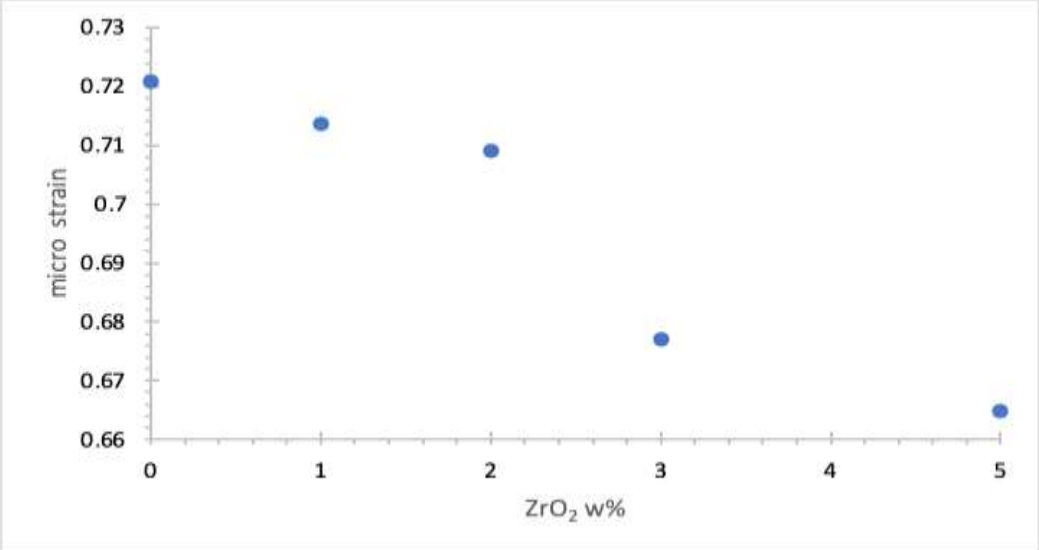

Fig.9:- Effect of ZrO_2 ratios on the micro strain of nano composite films.

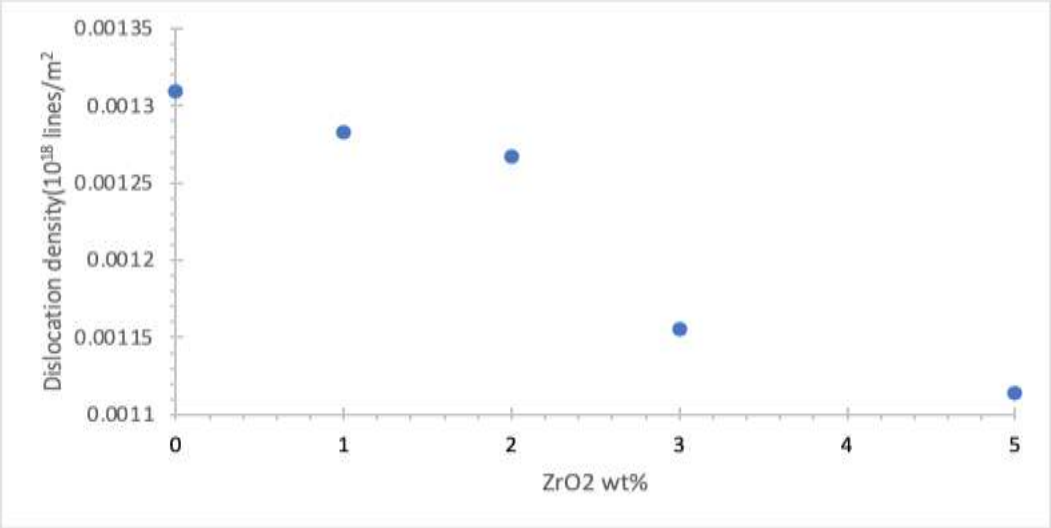

Fig.10:- Effect of ZrO_2 ratios on the dislocation density of nano composite films.

FTIR investigation

In order to illustrate the structure modification in prepared films of PVA due to addition ZrO2 with different ratios(1,2,3 and 5)wt.% FTIR was conducted. The indused modification were evaluated onsidering the variation the peak intensity that fits each function group. Figs (11-16) shows the FTIR spectra of PVA and PVA/$Zr0_2$ (wt.%) composite films were taken from 4000 to 350 cm^{-1}

Fig.11. shows the FTIR spectra (a) of PVA /$Zr0_2$ (0wt%) film.

Fig.12. shows the FTIR spectra (b) of PVA/$Zr0_2$ (1wt%) composite.

Fig.13. shows the FTIR spectra (c) of PVA/$Zr0_2$ (2wt%) composite.

Fig.14. shows the FTIR spectra (d) of PVA/$Zr0_2$ (3wt%) composite.

Fig.15. shows the FTIR spectra (e) PVA/$Zr0_2$ (5wt%) composite.

Fig.16. FTIR spectra of pure PVA and PVA/ZrO_2 composite Film with different ratios ZrO_2 (a - 0Wt% ZrO_2 , b -1Wt% ZrO_2 , c -2Wt% ZrO_2 , d -3Wt% ZrO_2, and e-5Wt% ZrO_2 5wt.%)

In the FTIR spectra of pure PVA as in fig.11. and table 3. show the main function groups observed at 3354 cm^{-1} are assigned to the O-H stretching vibration of PVA. Peaks at 2925 and 2854 cm^{-1} are corresponding to the CH, and CH symmetric stretching vibration, respectively. The peaks at 1650 and 1705 cm^{-1} attributed to absorption stretching mode of C=0 and C=C, respectively. The band observed at 1469 cm^{-1} is assigned to the stretching of the carbonyl group (C=0) and the band at 1435 cm ' corresponds to the symmetric banding mode (CH2). The peak at 1372 cm^{-1} is

attributed to mixed (CH and OH) bending modes. The peaks at 1235 $cm^{-1}$and 1100 cm^{-1} are corresponding to CH2 wagging vibrations, -CH2 stretching vibration, and C-O respectively.

In the FTIR spectra of PVA/ZrO_2 (5 wt%) (Fig.12.) composite film, the observed FTIR peaks are similar to the PVA peaks except new peaks at 725 cm^{-1} and small hump at 690cm^{-1} observed are categorized as the zirconium and oxygen (Zr-O) band stretching mode , which indicates the presence of ZrO_2, nanoparticles in the composite film and it's increased with increasing the ratio of ZrO_2.

Further, we observed that in the composite films, the slight broadening the peak center which corresponding to the O-H stretching vibration (3359cm-^{1}) and there is a remarkable decrease in the intensity of O-H stretching vibration that may be due to the hydrogen bonding between the oxygen of Zr ion of ZrO_2 and -OH group of PVA. Changes in intensity and slight shifts in peak positions of some bands indicate stronger interaction between the polymer and nanoparticles.

Additionally, we noticed that two peaks at 1753 cm^{-1} and 1666 cm^{-1} correspond to the stretching mode of C=0 and C=C were observed in PVA membrane, recombining into a single peak at 1714 cm^{-1} in the case of PVA/ZrO_2 which also revealed the stronger interaction between PVA and $ZrO_{2.}$ Nanoparticles similar results also reported by Waly et al[1].

Table 3:- FTIR functional group of PVA/$ZrO_{2.}$

Wave number cm^{-1}	Function group
3354 cm^{-1}	O-H stretching vibration of PVA
2925 and 2854 cm^{-1}	CH, and CH symmetric stretching vibration,
1650 cm^{-1}	attributed to absorption stretching mode of C=0
1705 cm^{-1}	attributed to absorption stretching mode C=C
1469 cm^{-1}	is assigned to the stretching of the carbonyl group (C=0)
1435 cm^{-1}	corresponds to the symmetric banding mode (CH2)
1372 cm^{-1}	is attributed to mixed (CH and OH) bending modes
1325 cm-1	assigned to H-C-H and C-O-H bending vibrations
1235 cm^{-}	are corresponding to CH2 wagging vibrations,
1100 cm^{-1}	-CH2 stretching vibration
827 cm^{-1}.	Corresponds to C-C stretching and also C-H out-of-plane vibrations
695 cm^{-1}	corresponds to the zirconium and oxygen (Zr-O) band stretching mode

Optical properties

The UV–Vis. spectra of PVA and PVA/ZrO_2 nanocomposites were recorded in the range of 190-800 nm. The spectra of pristine PVA and that of PVA substituted with different ZrO_2 concentrations (1, 2, 3, and 5 wt.%) are shown in fig.17. The absorption of PVA film increases with increasing the ZrO_2 content in both regions (UV and visible regions), where the PVA spectrum has one absorption band associated with a small shoulder like a band shown on a spectrum of pure PVA at approx. ~278.8 nm owing to π-π* transition corresponding to the C-C vibration. and this agree with. This shoulder exists with an irregular variation in position in the spectrum of pure PVA and 1 wt.%ZrO_2 films and almost gone in prepared films with high ratio of ZrO_2 as shown in figs.17.

In fig.18. shows that the optical transmission of studied composite films decreased rapidly by raising ZrO_2 content and becomes almost 90% UV light absorption for the composite film PVA/5 wt.% ZrO_2, this because ZrO_2 is considered an actively and typically photocatalyst and photon absorber among wide band metal oxides. Due to their configuration (Zr4+ ion is d0), d-d transitions cannot occur in the vision area Then, composite films are more absorbed with increasing ZrO_2 concentration. This is because the addition of ZrO_2 particles absorbs the radiation incident through its free electrons and this agree with This feature makes PVA films a prospective candidate for UV protection, which is preferred in the application for food packaging[4].

Fig.17. Effect of ZrO_2 ratios on the absorption (A%)of the composite PVA/ZrO_2 films
(a -0Wt% ZrO_2 , b -1Wt% ZrO_2 , c -2Wt% ZrO_2 , d -3Wt% $ZrO_{2,}$ and e-5Wt% ZrO_2 5wt.%)

Fig.18. UV–visible transmission spectra for different ratio of ZrO_2
(a -0Wt% ZrO_2 , b -1Wt% ZrO_2 , c -2Wt% ZrO_2 , d -3Wt% ZrO_2, and e-5Wt% ZrO_2 5wt.%)

Absorption edge
Equation 3 determines the absorption coefficient (α) as a function of wavelength, where
A is the absorbance at a specific wavelength and d is the sample thickness.

$$\alpha = (2.303*A)/d \qquad (3)$$

The optical absorption coefficient was determined as a function of the incident photon energy for pure PVA and substituted PVA (PVA/ZrO_2), as depicted in fig.19. From the Figure, the absorption edge of pure PVA has been shifted to the lower energy region with the increase of the ZrO_2 ratio.

Fig.19. also shows that as the photon energy increases, the absorption coefficient for all samples increases gradually. Such an increase is linked to the indirect energy gap. The redshift of the absorption edge observed in all samples refers to the bandgap energy decrease. This large shift in the absorption edge may be due to the formation of charge transfer in PVA[7].

The absorption edge E eV was determined by extrapolating the linear portion of the curves to zero absorption α = 0. It is obvious that the absorption coefficient increases as well as the absorption edge shifts to lower energy with the addition of ZrO_2. This indicates a decreasing in the gap of the optical band for the mixed doped films. The values obtained for the edge of absorption are tabulated in table 4. It may be obvious that the absorption edge for PVA is 5.2 eV and decreased to 3.2 eV for 5 wt.% ZrO_2/PVA film shows the creation of localized states in the forbidden gap and this agree with. Fig.19. also reveals that the absorption edge of natural PVA and composite PVA/ZrO_2 films have significant change due to completely incorporation between the PVA matrix and ZrO_2 particles and this confirmed by XRD results[4].

Fig.19. Relation between the absorption coefficient α and energy E=hυ of virgin PVA and. PVA/ZrO_2 films
(a -0Wt% ZrO_2 , b -1Wt% ZrO_2 , c -2Wt% ZrO_2 , d -3Wt% ZrO_2, and e-5Wt% ZrO_2 5wt.%)

Optical energy gap
Based on Davis and Mott model, the optical bandgap energy can be determined near the edge of fundamental absorption (300-800 nm) using the following equation:

$$(\alpha h\upsilon) = B(h\upsilon - Eg)^n \qquad (4)$$

where B is the constant associated with electronic transitions probabilities, hυ is the photon energy, Eg is the optical energy gap, and n is an exponent factor determine the type of electronic transitions that could occur during the process of photon absorption[4, 8]. For forbidden and allowed direct transition, n = 3/2 and ½, while for indirect n = 2 and 3, respectively. transitions can occur both directly and indirectly near the basic band edge. This is indicated by plotting $(\alpha h\upsilon)^{1/2}$ and $(\alpha h\upsilon)^2$ as a function of photon energy (hυ) . The point of crossing the linear regions in Figs(20-24) with the photon energy axis is assessed to the values of bandgap values. The variations in the electrical features of materials are known to arise from band structure. Knowledge of the band gaps is therefore extremely important.

The bandgap values for the permitted indirect and direct transitions are presented in Table.4. The bandgap values are shown to decline with the rising concentration of ZrO_2. The optical energy gap decreases from 3.36 eV for pure PVA to 2.4 eV for PVA/ZrO_2 composite film and from 4.62 eV for pure PVA to 2.9 eV for PVA/ZrO_2 composite film for direct and indirect bandgap, respectively. This reduction may be ascribed as the following mechanisms: defects in the PVA matrix generating localized states in the optical band gap reduce the bandgap, when ZrO_2 is inserted into the PVA matrix.

Formation of charge transfer complexes within the host matrix. As a consequence, the ZrO_2 molecules bridge the gap between the two localized states with an increase in ZrO_2 concentration, thus reducing the potential barrier between them. The bandgap reduction detected is influenced by all of the above factors. The decrease in the energy gap owing to the development of new levels in the bandgap facilitates the transition of electrons from the valence band to these local levels to the conductive band, thereby increasing the conductivity and decreasing the bandgap[4].

Table 4:- Optical parameters for pure PVA and composite films PVA/ZrO_2.

sample	E edge (eV)	Eg direct eV	Eg indirect eV	Eu ev
PVA	5.2	3.6	4.62	1.58
PVA/1 ZrO_2 W%	5	3.4	4.4	1.87
PVA/2 ZrO_2 W%	4.3	3.36	4.04	1.89
PVA/3 ZrO_2 W%	3.6	3.2	3.42	4.67
PVA/5 ZrO_2 W%	3.2	2.47	2.9	4.45

Fig.20a. Relation between the absorption coefficient (αhn)2 and energy E=hυ of virgin PVA.

Fig.20b. Relation between the absorption coefficient (αhn)0.5 and energy E=hυ PVA

Fig.21a. Relation between the absorption coefficient (αhn)2 and energy E=hυ of composite film with ratio 1% ZrO_2.

Fig.21b. Relation between the absorption coefficient (αhn)0.5 and energy E=hυ of composite film with ratio 1% ZrO_2.

Fig.22a. Relation between the absorption coefficient (αhn)2 and energy E=hυ of of composite film with ratio 2% ZrO_2.
.

Fig.22b. Relation between the absorption coefficient (αhn)0.5 and energy E=hυ of of composite film with ratio 2% ZrO_2.
.

Fig.23a. Relation between the absorption coefficient $(\alpha hn)^2$ and energy E=hυ . of composite film with ratio 3% ZrO_2.
of

Fig.23b. Relation between the absorption coefficient (αhn)0.5 and energy E=hυ of of composite film with ratio 3% ZrO_2.

.

Fig.24a. Relation between the absorption coefficient (αhn)2 and energy E=hυ of of composite film with ratio 5% ZrO_2.

Fig.24b. Relation between the absorption coefficient $(\alpha hn)^{0.5}$ and energy E=hυ of of composite film with ratio 5% ZrO_2.

.

Typical variation of band gap with crystallite size in the nanocomposite films is shown in Fig.25. which indicates an increase in the band gap with a decrease in crystallite size.

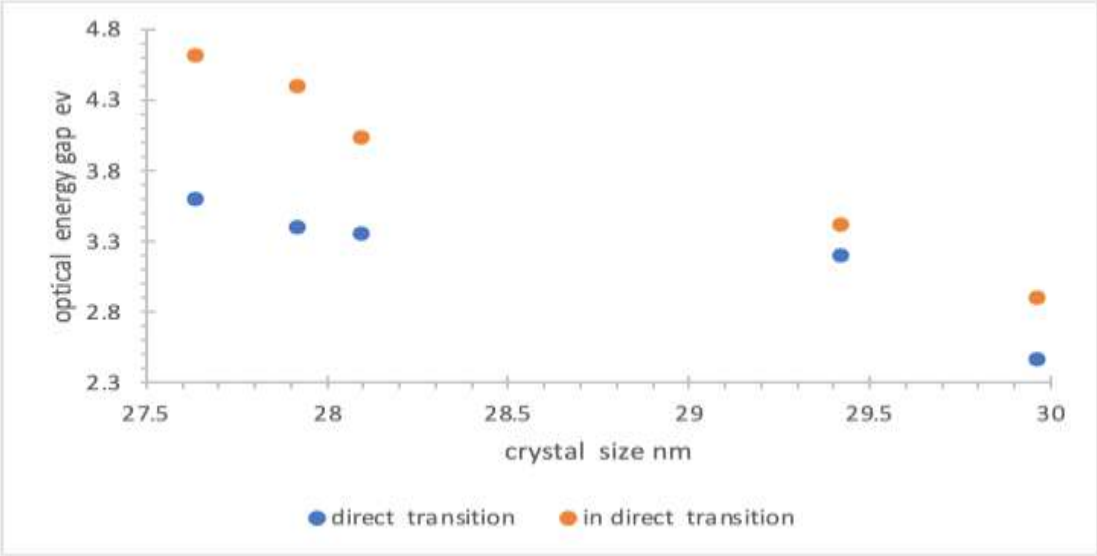

Fig.25:- The relation between crystal size and optical energy gab.

The Urbach energy (E_u)

The disordered materials have tail states in the gap area below the main absorption edge; these can be calculated from the absorption coefficient (α) following the Urbach rule ;

(5)

(6)

where is a constant that defines the matter, The Urbach energy (E_u) which refers to the width of the tail of localized states in the forbidden bandgap [9]. The value of (Eu) was evaluated by plotting ln(α) versus hν and taking the slope of linear portion as displayed in figs.26. The figure indicates the effect of ZrO_2 contents on the (Eu) of the prepared films. On increasing the ZrO_2 contents, Eu increased. On loading with 5 wt% ZrO_2 contents, the Eu value

shifted to 4.2 eV (from 1. 46 eV of pure PVA). The origin of (Eu) might be attributed to lattice thermal vibrations. The changes induced in band gap energy and band tail reveal that the energy states of pure PVA might be modified via incorporation of ZrO_2 filler. On introducing the filler into polymer matrix, it created localized states in the forbidden band that might change the Femi level. These states govern the optoelectrical attributes of the prepared nanocomposites films and play role of recombination and trapping centers. So on boosting the low energy transitions, the band gap narrowed, band tail width (Urbach energy) widened and the optoelectrical conductivity of the nanocomposites enhanced[10].

Fig.26a. Relation between the(lnα) of absorption coefficient and energy E=hυ of virgin PVA.

Fig.26b. Relation between the (lnα) of absorption coefficient and energy E=hυ of of composite film with ratio 1% ZrO_2.

Fig.26c. Relation between (lnα) of absorption coefficient and energy E=hυ of of composite film with ratio 2% ZrO_2.

Fig.26d. Relation between the (lnα) of absorption coefficient and energy E=hυ of composite film with ratio 3% ZrO_2.

Fig.26e. Relation between the (lnα) of absorption coefficient and energy E=hυ of of composite film with ratio 5% ZrO_2.

Refractive indices

The refractive indices, n of all the composites were calculated from the reflection and absorption spectra, in a range of wavelengths from 190 to 800 nm, by using the equation:

(7)

where R is the specular reflection, and k is the extinction coefficient corresponding to the imaginary part of the complex refractive index. Refractive index n of a material is a significant tool, because it is strongly linked to the local field inside the material and the electronic polarizability. It is an important parameter in designing the optical devices. Improving the value of refractive index for PVA increases its feasibility of usage on large scale in optical applications. The refractive index discloses how light travels through the material (medium). The imaginary part of refractive index is called extinction coefficient k.

The investigation of refractive index and extinction coefficient is essengthonitoring the optical systems. The optical losses are determined using extinction coefficients. The parameter extinction coefficient k is related to absorption coefficient α as:

k= /4 (8)

The values of reflectance R were acquired from absorption data. The variation trend of extinction coefficient k against wavelength λ (Fig.27a.) indicated the interaction between incident photons and the medium. The extinction coefficient is the measure of fractional loss of radiation energy because of scattering process in the medium. The

small value of extinction coefficient (~10^{-2}) in the figure depicts that the samples under investigation were translucent. Figure 27a shows the variation in refractive indices with respect to incident wavelength for the prepared films. It indicates that on increasing the ZrO_2 contents, the extinction coefficient and refractive index both shifted to higher values but the rise in extinction coefficient was smaller as compared to that in refractive index. The values of refractive index and extinction coefficient both decreased on increasing the incident wavelengths, and the trends of curves are consistent with that earlier reported work. It could also be observed that refractive indices of the nanocomposite films are more pronounced than that of pure PVA. Fig.27a. indicates that refractive indices of the samples in UV region are higher than those in visible region. The inset of Fig.27a. shows how refractive index varied with ZrO_2 contents, which means that refractive index was linearly raised from 1.3 (for pure PVA) to 1.4 (for 0.5 wt% ZrO_2-nanofilled PVA). Similar linear correlation between refractive index and ZrO_2 contents had been reported in the literature and designated as homogenous dispersion of ZrO_2 into the matrix. Thus, the values of extinction coefficients and refractive indices of the nanocomposite films could be tuned using variation in filler contents. The creation of localized states in the forbidden bands (due to filler incorporation) might be a reason for observed variation in refractive indices of nanocomposite films. The observed trend of extinction coefficient and refractive index with incident wavelength and ZrO_2 contents suggests their use in reflectors manufacturing industry[10].

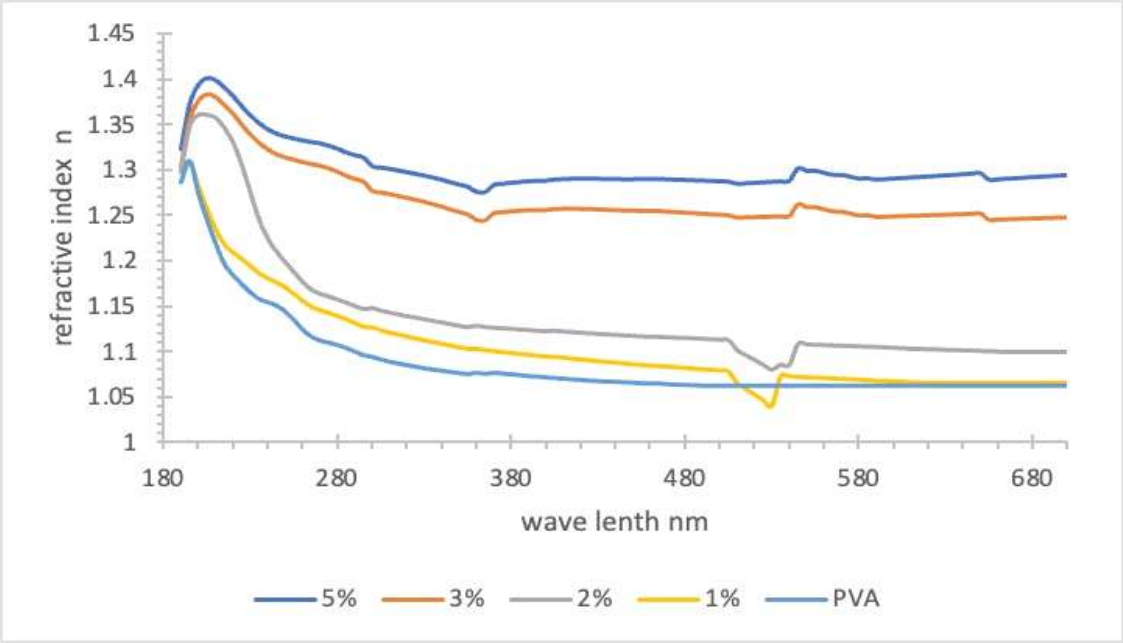

Fig.27a:- Relation between refractive index with wave engths for all prepared composite films. (a -0Wt% ZrO_2 , b -1Wt% ZrO_2 , c -2Wt% ZrO_2 , d -3Wt% ZrO_2, and e-5Wt% ZrO_2 5wt.%)

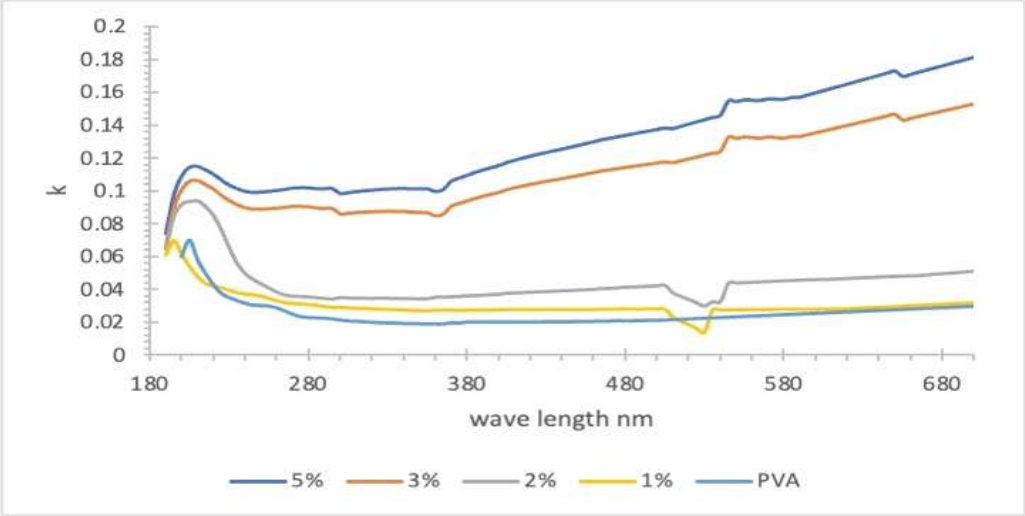

Fig.27b:- Relation between extension coefficient with wave length for all prepared composite films (a -0Wt% ZrO_2 , b -1Wt% ZrO_2 , c -2Wt% ZrO_2 , d -3Wt% ZrO_2, and e-5Wt% ZrO_2 5wt.%).

Optical conductivity

The optical conductivity (σ) was evaluated using equation: σ =nc/ 4 where c is the speed of light in vacuum. Fig.28. presents the variation in optical conductivity with incident wavelength for nano composite films. The optical conductivity of the fabricated nanocomposite films has higher values in UV region due to higher absorption of incident photon energy by the ZrO_2 in this region as compared to that in visible region. The figure shows that the optical conductivity in visible region gradually decreases and then becomes constant. A feeble value of optical conductivity in visible region shows very poor electronic excitation of incident photons in that region. Due to good absorption of UV photons, the prepared nanocomposite films might be used as UV absorbers (filters). The figure indicates that the optical conductivity increases on adding more contents of ZrO_2 nanofillers up to 5wt%[10].

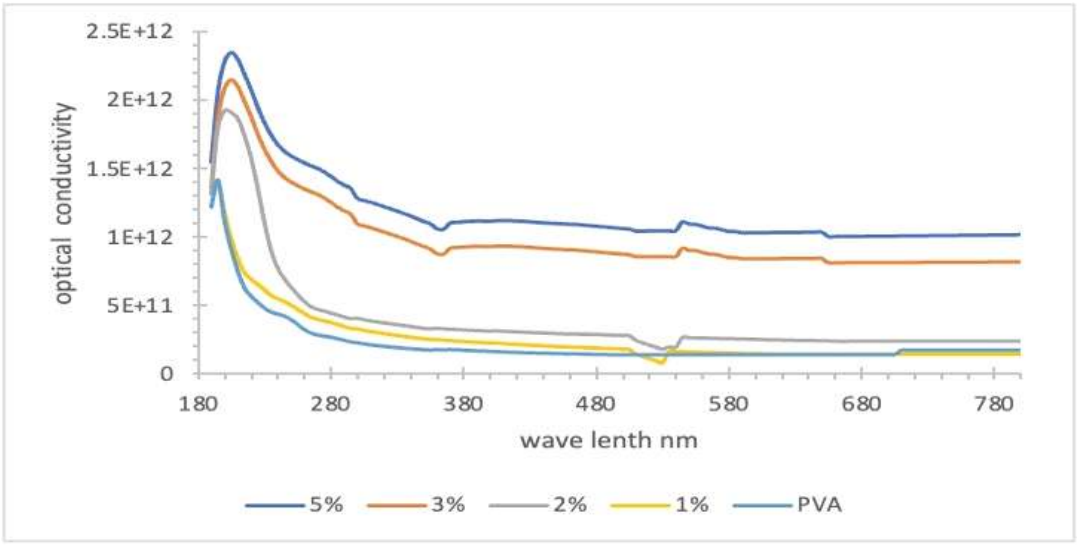

Fig.28:- Relation between optical conductivity with wave length for all prepared composite film (a -0Wt% ZrO_2 , b -1Wt% ZrO_2 , c -2Wt% ZrO_2 , d -3Wt% ZrO_2, and e-5Wt% ZrO_2 5wt.%)

Conclusion:-

PVA/ZrO_2 nanocomposites and ZrO_2 have identical crystalline lattices, ZrO_2 does not affect the main crystal structure of PVA. At low concentrations.

The XRD patterns of the films exhibited characteristic diffraction peaks corresponding to the crystalline structure of PVA and ZrO_2. The intensity of the diffraction peaks varied with the addition of ZrO_2 nanoparticles, indicating changes in the crystallinity of the composite films. The peak intensities and the decrease of broadened with increasing ZrO_2 content, suggesting a improvement of PVA crystallinity. This could be attributed to the disruption of PVA crystalline regions by the presence of ZrO_2 nanoparticles. Typical variation of band gap with crystallite size in the nanocomposite films which indicates an increase in the band gap with a decrease in crystallite size.

Due to configuration of (Zr4+ ion is d0), the composite films are more absorbed with increasing ZrO_2 concentration. This is because the addition of ZrO_2 particles absorbs the radiation incident through its free electrons and this agree with This feature makes PVA films a prospective candidate for UV protection, which is preferred in the application for food packaging.

The effect of varying amounts of ZrO_2 nanoparticles on the structural and optical characteristics of composites has been explored to assess a suitable material for optical and optoelectronic applications.

Due to good absorption of UV photons, the prepared nanocomposite films might be used as UV absorbers (filters). The figure indicates that the optical conductivity increases on adding more contents of ZrO_2 nanofillers up to 0.5 wt%. films with enhanced optomechanical properties

References:-

1. Mehto, A., V.R. Mehto, and J. Chauhan, Preparation and Characterization of Polyvinyl Alcohol (PVA)/ZrO2 Composite Membranes. physica status solidi (b), 2023. **260**(10): p. 2300164.
2. Mallakpour, S. and A. Nezamzadeh Ezhieh, Polymer nanocomposites based on modified ZrO2 NPs and poly (vinyl alcohol)/poly (vinyl pyrrolidone) blend: optical, morphological, and thermal properties. Polymer-Plastics Technology and Engineering, 2017. **56**(10): p. 1136-1145.
3. Tharani, S.S.N., Green synthesis of zirconium dioxide (ZrO2) nano particles using Acalypha indica leaf extract. International Journal of Engineering and Applied Sciences, 2016. **3**(4): p. 257689.
4. Khairy, Y., et al., The optical characteristic of PVA composite films doped by ZrO2 for optoelectronic and block UV-Visible applications. Materials Research Express, 2019. **6**(11): p. 115346.
5. Guerbous, L., Structural and Optical Properties of Pva/Zro2: Eu3+ Hybrid Films Prepared Via Γ-Irradiation.
6. Begum, A., A. Hussain, and A. Rahman, Effect of deposition temperature on the structural and optical properties of chemically prepared nanocrystalline lead selenide thin films. Beilstein Journal of Nanotechnology, 2012. **3**(1): p. 438-443.
7. Badry, R., et al., Effect of zinc oxide on the optical properties of polyvinyl alcohol/graphene oxide nanocomposite. Biointerface Res. Appl. Chem, 2023. **13**(39): p. 2022.
8. Zeng, F., et al., Insight into the Effect of Selenization Temperature for Highly Efficient Ni-Doped Cu2ZnSn (S, Se) 4 Solar Cells. Nanomaterials, 2022. **12**(17): p. 2942.
9. Gharbi, F., et al., Structural, Thermal, and Optical Studies of Gamma Irradiated Polyvinyl Alcohol-, Lignosulfonate-, and Palladium Nanocomposite Film. Polymers 2022, 14, 2613. 2022, s Note: MDPI stays neutral with regard to jurisdictional claims in published ….
10. Aslam, M., M.A. Kalyar, and Z.A. Raza, Fabrication of nano-CuO-loaded PVA composite films with enhanced optomechanical properties. Polymer Bulletin, 2021. **78**: p. 1551-1571.